Available online at www.sciencedirect.com

ScienceDirect

Nuclear Physics B 956 (2020) 115013

NUCLEAR PHYSICS B

www.elsevier.com/locate/nuclphysb

Exclusive Z^0 photoproduction at the Large Hadron Collider and the Future Circular Collider

R.O. Coelho, V.P. Gonçalves *

Instituto de Física e Matemática, Universidade Federal de Pelotas, Caixa Postal 354, CEP 96010-900, Pelotas, RS, Brazil

Received 20 December 2019; received in revised form 1 April 2020; accepted 6 April 2020
Available online 10 April 2020
Editor: Tommy Ohlsson

Abstract

In this paper we present a comprehensive analysis of the exclusive Z^0 photoproduction in pp, pPb and $PbPb$ collisions for the energies of the Large Hadron Collider (LHC) and of the proposed Future Circular Collider (FCC). The rapidity distributions and cross sections are estimated considering the color dipole formalism and different phenomenological models for the gluon saturation effects. Our results indicate that the exclusive Z^0 photoproduction in pp collisions at the FCC will be sensitive to the description of the non-linear effects in the QCD dynamics.

1. Introduction

The experimental study of photon – induced interactions in $pp/pA/AA$ collisions became a reality in the last years [1–13], strongly motivated by the possibility of constraining the dynamics of the strong interactions at large energies (for a recent review see Ref. [14]). One of most promising observables is the exclusive vector meson photoproduction cross section [15,16], which is driven by the gluon content of the target (proton or nucleus) and is strongly sensitive to non-linear effects (parton saturation) [17]. Such expectation has motivated the analysis of exclusive ρ, ϕ, J/Ψ, $\Psi(2S)$ and Υ photoproduction in pp, pA and AA collisions at RHIC and

* Corresponding author.
E-mail address: barros@ufpel.edu.br (V.P. Gonçalves).

https://doi.org/10.1016/j.nuclphysb.2020.115013
0550-3213/

LHC energies considering different theoretical approaches for the treatment of the QCD dynamics and for the vector meson wave function (see, e.g., Refs. [18–27]). In particular, the recent study performed in Ref. [23] indicated that a global analysis of the experimental RHIC and LHC data for the rapidity distributions of all these different final states will be necessary to discriminate between the distinct theoretical approaches. As a consequence, the analysis of other final states is important and timely. One alternative is the study of the $\gamma p \to Z^0 p$ reaction, which was studied for the first time in Ref. [28] considering the two - gluon exchange model for the QCD Pomeron. Such analysis was extended for pp and $PbPb$ collisions in Ref. [29] taking into account of the higher – order corrections to the QCD Pomeron and improved in Refs. [30,31] for the case of pp collisions. As in the case of vector meson production, the cross section is proportional to the square of the gluon distribution (in the collinear formalism) [15], being thus strongly dependent on the description of the QCD dynamics at high energies. The results presented in the Refs. [29–31] indicated that the experimental analysis of this final state is, in principle, feasible in hadronic collisions at high energies. It is important to emphasize that the CDF Collaboration [32] searched the exclusive Z^0 photoproduction in pp collisions at $\sqrt{s} = 1.96$ TeV and derived an upper bound for the cross section.

In this paper we will present an updated and improved analysis of the exclusive Z^0 photoproduction in pp, pPb and $PbPb$ collisions. One of the goals of this paper is to improve the study performed in Ref. [29] by taking into account the corrections to the overlap function between the photon and Z^0 wave functions associated to the fact that the outgoing Z^0 has a timelike virtuality $q^2 = M_Z^2 > 0$. Second, to present updated predictions for pp and $PbPb$ collisions derived using the more recent phenomenological models for the dipole – proton scattering amplitude, which describe the precise HERA data for inclusive and exclusive observables and take into account the corrections associated to the DGLAP evolution, which are important for the description of the Z^0 photoproduction. Finally, we will present, for the first time, predictions for pPb collisions at the LHC energy as well as for pp, pPb and $PbPb$ collisions at the energies of the proposed Future Circular Collider (FCC) [33–35]. For the LHC, the maximum photon – nucleon center – of – mass energy, $W_{\gamma N}^{\max}$, reached in $pp/pPb/PbPb$ collisions at $\sqrt{s} = 14/8.8/5.5$ TeV is $8.4/1.5/0.95$ TeV [36]. On the other hand, for the FCC we will reach $W_{\gamma N}^{\max} \approx 55/8.7/6.8$ TeV for $pp/pPb/PbPb$ collisions at $\sqrt{s} = 100/63/39$ TeV. Therefore, the FCC will probe an unexplored range of photon – hadron center – of – mass energies, where the contribution of non – linear effects for the QCD dynamics are expected to modify the behavior of the observables, as demonstrated e.g. in Ref. [37] for the case of the exclusive vector meson photoproduction in pp collisions at the FCC energy.

The paper is organized as follows. In Sec. 2 we present a brief review of the color dipole formalism and the main expressions used to estimate the exclusive Z^0 photoproduction. Moreover, the distinct models for the dipole – hadron scattering amplitude are discussed. In Sec. 3, we present our predictions for the cross sections and rapidity distributions to be measured in $pp/pPb/PbPb$ collisions at the LHC and FCC energies. Finally, in Sec. 4, we summarize our main conclusions.

2. Formalism

The exclusive Z^0 photoproduction in ultraperipheral hadronic collisions is represented by the diagrams shown in Fig. 1. We will consider ultraperipheral collisions (UPCs), which are defined as collisions between two electric charges at large impact parameters $b > R_1 + R_2$, where R_i is the radius of the charge i. In a UPC at high energies, it is well known that the hadrons act as a

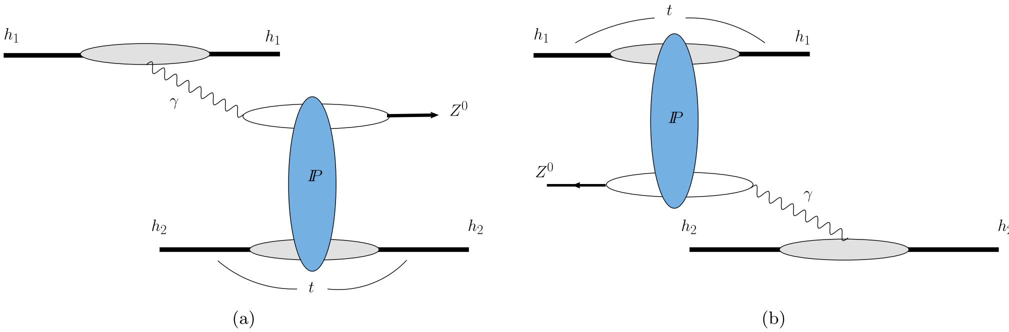

Fig. 1. Exclusive Z^0 photoproduction in (a) photon – Pomeron and (b) Pomeron – photon interactions at hadronic collisions.

source of almost real photons [36]. Consequently, in the case of the exclusive Z^0 photoproduction we must take into account the contributions associated to photon - Pomeron and Pomeron - photon interactions, represented in the Figs. 1 (a) and (b), respectively, where the Pomeron ($I\!P$) represents a color singlet exchange between the dipole and the target. The final state will be characterized by two intact hadrons and two rapidity gaps, *i.e.* the outgoing particles are separated by a large region in rapidity in which there is no additional hadronic activity observed in the detector. Moreover, the hadronic cross section can be written in a factorized form, given by the so called equivalent photon approximation [38], with the differential cross section being expressed as follows

$$\frac{d\sigma\left[h_1+h_2\rightarrow h_1\otimes Z^0\otimes h_2\right]}{dY\,dt}=n_{h_1}(\omega_1)\cdot\frac{d\sigma}{dt}(\gamma h_2\rightarrow Z^0\otimes h_2)+n_{h_2}(\omega_2)\cdot\frac{d\sigma}{dt}(\gamma h_1\rightarrow Z^0\otimes h_1)\;, \quad (1)$$

where the rapidity (Y) of the Z^0 in the final state is determined by the photon energy ω in the collider frame and by the boson mass M_{Z^0} [$Y\propto\ln(\omega/M_{Z^0})$]. Moreover, $d\sigma/dt$ is the differential cross section of the $\gamma h\rightarrow Z^0\otimes h$ process, with the symbol $\otimes$ representing the presence of a rapidity gap in the final state, and $\omega_1\propto\exp(Y)$ [$\omega_2\propto\exp(-Y)$] is the energy of the photon emitted by the hadron h_1 (h_2). Furthermore, $n_h(\omega)$ denotes the equivalent photon spectrum of the relativistic incident hadron, with the flux of a nucleus being enhanced by a factor Z^2 in comparison to the proton one. It is important to emphasize that we are assuming that the photons emitted by hadrons are coherently radiated by the whole hadron. Such condition imposes that the minimum photon wavelength must be greater than the hadron radius. In other words, the photon virtuality must satisfy $Q^2=-q^2\leq 1/R_h^2$, with the photon four – momentum being $q^\mu=(\omega,\vec{q_\perp},q_z=\omega/v)$, where $\vec{q_\perp}$ is the transverse momentum of the photon in a given frame, where the projectile moves with velocity v. Therefore, we have that $Q^2=\omega^2/\gamma_L^2+q_\perp^2$. The coherence condition limits the maximum energy of the photon to $\omega<\omega_{\rm max}\approx\gamma_L/R_h$ and the perpendicular component of its momentum to $q_\perp\leq 1/R_h$. As a consequence, the coherence condition sets an upper limit on the transverse momentum of the photon emitted by the hadron, which should satisfy $q_\perp\leq 1/R_h$, being $\approx 28\,(330)$ MeV for $Pb\,(p)$ beams. Therefore, the photon virtuality can be neglected and the photons can be considered as being real. The maximum photon energy can also be derived considering that the maximum possible momentum in the longitudinal direction is modified by the Lorentz factor, γ_L, due to the Lorentz contraction of the hadrons in that direction.

It implies $\omega_{\max} \approx \gamma_L/R_h$ and, consequently, $W_{\gamma N}^{\max} = \sqrt{2\,\omega_{\max}\sqrt{s}}$. Considering the values for $pp/pPb/PbPb$ collisions at the LHC and FCC energies we can derive the values of $W_{\gamma N}^{\max}$ quoted in the previous Section, which are greater than the threshold energy for the production of a Z^0 in the final state. The coherence condition is taken into account in the calculation of the photon spectrum associated to the proton and nucleus, which we will describe using the Dress - Zeppenfeld [39] and the relativistic point – like charge [36] models, respectively. Moreover, in our analysis we will not consider the incoherent Z^0 photoproduction, $\gamma h \rightarrow Z^0 h^*$, where the target dissociates in the diffractive interaction. As demonstrated, e.g. in Refs. [40–43] for the case of the vector meson photoproduction, such contribution only becomes important at large $-t$.

The differential cross section for the $\gamma h \rightarrow Z^0 \otimes h$ process is given by

$$\frac{d\sigma}{dt} = \frac{1}{16\pi}|\mathcal{A}^{\gamma h \rightarrow Z^0 h}(x,\Delta)|^2\,, \tag{2}$$

where $|t|$ is the squared transverse momentum of the Z^0 in the final state and $\mathcal{A}$ is the amplitude for producing a Z^0 diffractively. In the color dipole formalism [44], this amplitude can be factorized in terms of the fluctuation of the virtual photon into a $q\bar{q}$ color dipole, the dipole-hadron scattering by a color singlet Pomeron exchange (denoted $I\!P$ in Fig. 1) and the recombination of the $q\bar{q}$ pair into the gauge boson Z^0. Consequently, the amplitude can be expressed as follows [45]

$$\mathcal{A}^{\gamma h \rightarrow Z^0 h}(x,\Delta) = i\int dz\, d^2\boldsymbol{r}\, d^2\boldsymbol{b}_h\, e^{-i[\boldsymbol{b}_h - \frac{1}{2}(1-2z)\boldsymbol{r}].\boldsymbol{\Delta}} \sum_f (\Psi^{Z*}\Psi)_T^f\; 2\mathcal{N}^h(x,\boldsymbol{r},\boldsymbol{b}_h)\,, \tag{3}$$

where $\Delta = \sqrt{-t}$ is the momentum transfer, $\boldsymbol{b}_h$ is the impact parameter of the dipole relative to the hadron target, and the variables $\boldsymbol{r}$ and z are the dipole transverse pair separation and the momentum fraction of the photon carried by a quark (an antiquark carries then $1-z$), respectively. Moreover, $(\Psi^{Z*}\Psi)_T^f$ denotes the transversely polarized overlap function between the photon and the Z^0 wave functions for a given quark flavor f. In our analysis we will sum over the quark flavors $f = u, d, s, c, b$. As in Ref. [30] we will take into account that the outgoing Z^0 has a timelike virtuality $q^2 = M_Z^2 > 0$, which implies that the overlap function is not the same derived from the application of the color dipole model to charged-current deep-inelastic scattering (see, e.g. Ref. [46]). Moreover, we also will include the contributions associated to the real part of amplitude and to the skewedness effect (for details see, e.g. Ref. [30]).

The function $\mathcal{N}^h(x,\boldsymbol{r},\boldsymbol{b}_h)$ in Eq. (3) is the forward dipole-hadron scattering amplitude (for a dipole at impact parameter $\boldsymbol{b}_h$) which encodes all the information about the hadronic scattering. It depends on the γh center - of - mass reaction energy, $W = [2\omega\sqrt{s}]^{1/2}$, through the variable $x = M_Z^2/W^2$. One of the main open questions in QCD is the treatment of its high energy regime, where non – linear (gluon saturation) effects are expected to contribute [17]. Currently, the bCGC and IP-SAT models, which are based on different assumptions for the treatment of the gluon saturation effects, and describe with success the high precision HERA data for inclusive and exclusive *ep* processes. In the impact parameter Color Glass Condensate (bCGC) model [47] the dipole - proton scattering amplitude is given by

$$\mathcal{N}^p(x,\boldsymbol{r},\boldsymbol{b}_p) = \begin{cases} \mathcal{N}_0 \left(\frac{r\,Q_s(b_p)}{2}\right)^{2\left(\gamma_s + \frac{\ln(2/r\,Q_s(b_p))}{\kappa\,\lambda\,y}\right)} & r\,Q_s(b_p) \leq 2 \\ 1 - e^{-A\,\ln^2(B\,r\,Q_s(b_p))} & r\,Q_s(b_p) > 2\,, \end{cases} \tag{4}$$

with $\kappa = \chi''(\gamma_s)/\chi'(\gamma_s)$, where χ is the LO BFKL characteristic function and $y = \ln(1/x)$. The coefficients A and B are determined uniquely from the condition that $\mathcal{N}^p(x,\boldsymbol{r},\boldsymbol{b}_p)$, and its derivative with respect to $r\,Q_s(b_p)$, are continuous at $r\,Q_s(b_p) = 2$. The impact parameter dependence of the proton saturation scale $Q_s(b_p)$ is given by:

$$Q_s(b_p) \equiv Q_s(x, b_p) = \left(\frac{x_0}{x}\right)^{\frac{\lambda}{2}} \left[\exp\left(-\frac{{b_p}^2}{2B_{\rm CGC}}\right)\right]^{\frac{1}{2\gamma_s}}, \tag{5}$$

with the parameter $B_{\rm CGC}$ being obtained by a fit of the t-dependence of exclusive J/ψ photoproduction. The factors $\mathcal{N}_0$ and γ_s were taken to be free. In what follows we consider the set of parameters obtained in Ref. [48] by fitting the recent HERA data on the reduced ep cross sections: $\gamma_s = 0.6599$, $\kappa = 9.9$, $B_{CGC} = 5.5$ GeV^{-2}, $\mathcal{N}_0 = 0.3358$, $x_0 = 0.00105$ and $\lambda = 0.2063$. In the bCGC model, the saturation regime, where $r\,Q_s(b_p) > 2$, is described by the Levin - Tuchin law [49] and the linear one by the BFKL dynamics near of the saturation line. On the other hand, in the IP-SAT model [50], $\mathcal{N}^p$ has an eikonalized form and depends on a gluon distribution evolved via DGLAP equation, being given by

$$\mathcal{N}^p(x, \boldsymbol{r}, \boldsymbol{b}_p) = 1 - \exp\left[-\frac{\pi^2 r^2}{2N_c}\alpha_s(\mu^2)\; xg\left(x, \frac{C}{r^2} + \mu_0^2\right)\; T_G(b_p)\right], \tag{6}$$

with a Gaussian profile

$$T_G(b_p) = \frac{1}{2\pi B_G}\exp\left(-\frac{b_p^2}{2B_G}\right) \tag{7}$$

The constant C is a free parameter of the model and the initial gluon distribution, evaluated at μ_0^2, is taken to be $xg(x, \mu_0^2) = A_g x^{-\lambda_g}(1-x)^6$. In this work we assume the parameters obtained in Ref. [51]. As in the bCGC model, the IP-SAT predicts the saturation of $\mathcal{N}^p$ at high energies and/or large dipoles, but the approach to this regime is not described by the Levin - Tuchin law. Moreover, in contrast to the bCGC model, the IP-SAT takes into account the effects associated to the DGLAP evolution, which are expected to be important in the description of small dipoles. Consequently, both models are based on different assumptions for the linear and non - linear regimes. As pointed above, the current high precision HERA data are not able to discriminate between these models. In what follows we analyze the impact of these distinct models for the gluon saturation effects on the exclusive Z^0 photoproduction in hadronic collisions. For comparison, we also will present the predictions derived assuming that $\mathcal{N}^p(x, \boldsymbol{r}, \boldsymbol{b}_p)$ is given by the linear part of the IP-SAT model, denoted hereafter IP-NONSAT, which is

$$\mathcal{N}^p(x, \boldsymbol{r}, \boldsymbol{b}_p) = \frac{\pi^2 r^2}{2N_c}\alpha_s(\mu^2)\; xg\left(x, \frac{C}{r^2} + \mu_0^2\right)\; T_G(b_p), \tag{8}$$

with the parameters obtained in Ref. [51]. It is important to emphasize that due to the large mass of the Z^0, the $q\overline{q}$ dipole is spatially compact, which implies that the cross section is dominated by small pair separations. Therefore, we expect, in principle, a small contribution of the saturation effects and a large impact of the corrections associated to the DGLAP evolution. However, the impact of the saturation effects is determined by the saturation scale Q_s which depends of the value of Bjorken x variable probed in the process. At larger photon – hadron center – of – mass energies (smaller values of x) we have that the onset of the saturation effects occurs at smaller values of the dipole separation. Such conclusion can be verified in Fig. 2, where we present the dependence on r^2 of the forward dipole – proton scattering amplitude for two different values of x. We have that the description of the linear regime (small - r^2) is distinct in the bCGC and IP-SAT models, as well the transition between the linear and non – linear regimes, with the onset of

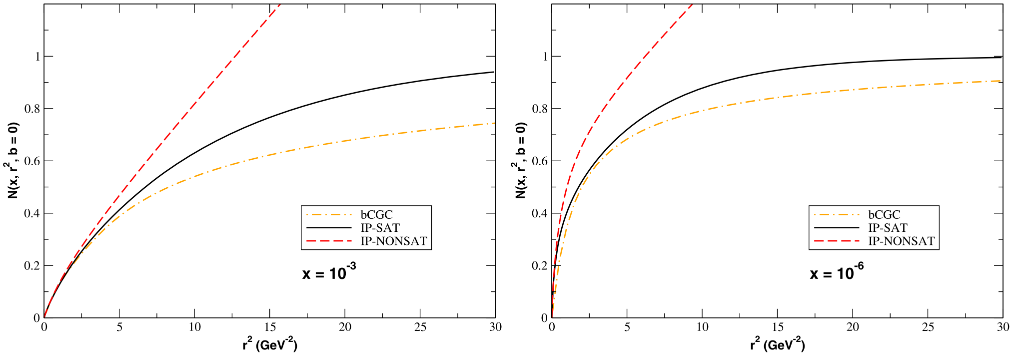

Fig. 2. Dependence on r^2 of the forward dipole – proton scattering amplitude for $b = 0$ and two values of the Bjorken – x variable predicted by the IP-SAT, IP-NONSAT and bCGC models.

the saturation regime ($\mathcal{N}^p \approx 1$) being slower in the case of the bCGC model. Another important aspect is that the contribution of large dipoles for the exclusive cross sections is larger than in inclusive processes, as demonstrated e.g. in Refs. [52,53]. One has that in exclusive processes, the main contribution comes from compact dipoles of small size, but the contribution of larger dipoles is not negligible. Such large dipoles are sensitive to the saturation effects, as observed in Fig. 2. As we will demonstrate below, for the photon – proton center – of – mass energies reached at the LHC, the typical values of x are not so small and, consequently, the contribution of the saturation effects is small. However, for FCC energies, the impact of the saturation effects on the exclusive Z^0 photoproduction become non - negligible due to the very small values of x probed in this case. A comment is in order here. A non-negligible contribution of the saturation effects for a cross section dominated by small dipoles is not unexpected. Previous phenomenological studies of the neutrino – nucleon cross section, which is dominated by $Q^2 \approx M_G^2$ ($G = Z^0, W^+, W^-$), already have observed that the saturation effects become important for very high neutrino energies [54–57]. Moreover, the theoretical studies performed in Ref. [58] have demonstrated that the saturation effects are important not only for $Q^2 < Q_s^2$, but in a much larger kinematical range, where $Q^2 \gg Q_s^2$, with the cross sections satisfying the geometric scaling property. The results obtained in Ref. [59] have show that the small-x HERA data for $Q^2 \leq 450\,\text{GeV}^2$ satisfy this property.

How to treat the dipole - nucleus interaction is still an open question due to the complexity of the impact parameter dependence. In principle, it is possible to adapt the phenomenological models described above to the nuclear case (see e.g. Refs. [24,53,60,61]). In what follows, we will assume the model proposed in Ref. [24], which includes the impact parameter dependence and describes the existing experimental data on the nuclear structure function [62]. In this model the dipole-nucleus scattering amplitude is given by

$$\mathcal{N}_A(x, \boldsymbol{r}, \boldsymbol{b}_A) = 1 - \exp\left[-\frac{1}{2}\sigma_{dip}(x, r^2)\, T_A(\boldsymbol{b}_A)\right], \tag{9}$$

where

$$\sigma_{dip}(x, r^2) = 2\int d^2\boldsymbol{b}_p\, \mathcal{N}_p(x, \boldsymbol{r}, \boldsymbol{b}_p), \tag{10}$$

and $T_A(\boldsymbol{b}_A)$ is the nuclear thickness, which is obtained from a 3-parameter Fermi distribution for the nuclear density normalized to A. The above equation sums up all the multiple elastic rescattering diagrams of the $q\overline{q}$ pair and is justified for large coherence length, where the transverse separation $\boldsymbol{r}$ of partons in the multiparton Fock state of the photon becomes a conserved quantity, *i.e.* the size of the pair $\boldsymbol{r}$ becomes eigenvalue of the scattering matrix. In what follows we will estimate the non – linear effects in the nuclear case by computing $\mathcal{N}_A$ considering as input in the calculations of the dipole - proton cross section the IP-SAT and bCGC models for the dipole - proton scattering amplitude discussed before. For comparison, we also will present the predictions derived assuming that the dipole – nucleus scattering amplitude is given by

$$\mathcal{N}_A(x,\boldsymbol{r},\boldsymbol{b}_A) = \frac{\pi^2 r^2}{2N_c}\alpha_s(\mu^2)\, xg\left(x, \frac{C}{r^2}+\mu_0^2\right)\, T_A(b_A)\,, \tag{11}$$

which is the generalization of the IP-NONSAT model for the nuclear case [51].

3. Results

In what follows, we will present our results for the cross sections and rapidity distributions of Z^0 gauge bosons produced in ultraperipheral pp, pPb and $PbPb$ collisions at the LHC and FCC energies. In our predictions we did not consider the corrections associated to soft interactions which would destroy the rapidity gaps [31] and, in the nuclear case, we did not include possible gluon shadowing corrections [21]. The treatment of both corrections is still is a theme of debate. In principle, these two corrections are expected to imply a small reduction of the cross sections for the case of the Z^0 photoproduction. It is important to emphasize that the results for the exclusive vector meson photoproduction presented in Ref. [23] indicate that the exclusive processes in ultraperipheral collisions can be described disregarding the gap survival corrections. In the color dipole formalism, the main open question present in the calculation of $\gamma h \to Z^0 h$ cross section is associated to the treatment of $\mathcal{N}^h(x,\boldsymbol{r},\boldsymbol{b}_h)$, since the overlap function $(\Psi^{Z*}\Psi)_T^f$ can be fully determined using electroweak theory (see Appendix A in Ref. [30]). In contrast, for the case of the exclusive vector meson photoproduction, the predictions are strongly dependent on the model assumed for the vector meson wavefunction (see, e.g. Ref. [23]), which should be estimated assuming a phenomenological model. Such aspect motivates the calculation of the exclusive Z^0 photoproduction assuming distinct models for the forward dipole – hadron scattering amplitude.

Initially let's consider pp collisions at $\sqrt{s} = 14$ and 100 TeV. In Fig. 3 (left panels) we present the photon – Pomeron and Pomeron – photon contributions, as well as the sum of them, derived using the IP-SAT model. From Eq. (1) we have that the behavior of the rapidity distribution for the photon – Pomeron contribution is determined by the photon flux for a photon with an energy $\omega \propto e^Y$ and the exclusive Z^0 photoproduction cross section for a given photon – proton center – of – mass energy W. While $\sigma_{\gamma h \to Z^0 h}$ increases with W, the photon flux strongly decreases when the photon energy is of the order $\omega_{\rm max} \approx \gamma_L/R_p$, becoming almost zero for larger photon energies. It explains why the rapidity distribution becomes zero at very large Y. Similar behavior is observed for the Pomeron – photon contribution, but in this case $\omega \propto e^{-Y}$. As expected, the rapidity distributions associated to the sum of the photon – Pomeron and Pomeron – photon contributions are symmetric with respect to $Y = 0$. We have that the distribution at midrapidities increases with the energy by a factor ≥ 3. Moreover, for the FCC energy, the exclusive Z^0 photoproduction at large rapidities ($2 \leq |Y| \leq 4$) is non - negligible. In Fig. 3 (right panels) we present our predictions considering the different models for the treatment of the dipole – proton scattering amplitude. We have that the bCGC model predicts the smaller values for the rapidity distributions. On the other hand, the IP-SAT and IP-NONSAT models, which taken into account

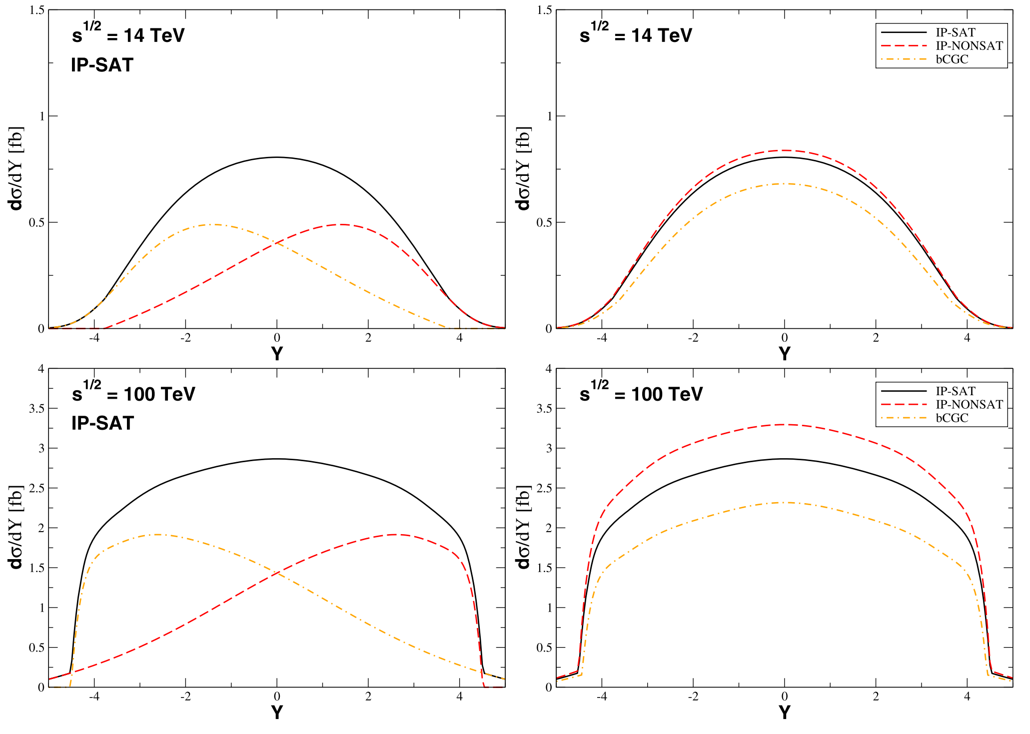

Fig. 3. Rapidity distributions for the exclusive Z^0 photoproduction in pp collisions at the LHC (upper panels) and FCC (lower panels) energies. Right panels: Comparison between the predictions derived using the different color dipole models; Left panels: The photon - Pomeron (red dashed) and Pomeron - photon (orange dot-dashed) contributions for the rapidity distributions. The black solid line represents the sum of both contributions. (For interpretation of the colors in the figures, the reader is referred to the web version of this article.)

the DGLAP evolution at small dipoles, predict similar values for the LHC energy. In contrast, for the FCC energy, the saturation effects included in the IP-SAT model implies a reduction of 10% at midrapidities, which is expected since the onset of the saturation effects occurs at smaller dipoles at larger energies.

In Fig. 4 we present our predictions for the exclusive Z^0 photoproduction in $PbPb$ collisions at $\sqrt{s} = 5.5$ and 39 TeV. The bCGC and IPSAT predictions are calculated using Eq. (9), while the IP-NONSAT one is estimated using Eq. (11). As in the case of pp collisions, the rapidity distributions are symmetric with respect to $Y = 0$. However, for $PbPb$ collisions, we have the rapidity distribution for the photon – Pomeron contribution becomes zero at smaller rapidities in comparison to the values observed in pp collisions. This behavior is associated to the fact that the Lorentz factor γ_L is smaller for a Pb beam and $R_{Pb} > R_p$. Consequently, the value of $\omega_{\max} \approx \gamma_L/R_h$, where the rapidity distribution for the photon – Pomeron strongly decreases, is smaller for $PbPb$ collisions in comparison to pp one. For $PbPb$ collisions, we predict cross sections of the order of pb instead of fb. This enhancement is directly associated to the Z^2 dependence of the nuclear photon flux, as well to the fact that $\sigma(\gamma A \rightarrow Z^0 A) \approx A \times \sigma(\gamma p \rightarrow Z^0 p)$. However, it is important to emphasize that the maximum photon – hadron center – of – mass energy reached in $PbPb$ collisions is smaller than in pp collisions, since that maximum photon energy is proportional to the Lorentz factor of the incident hadron and inversely proportional to its radius [36]. As a conse-

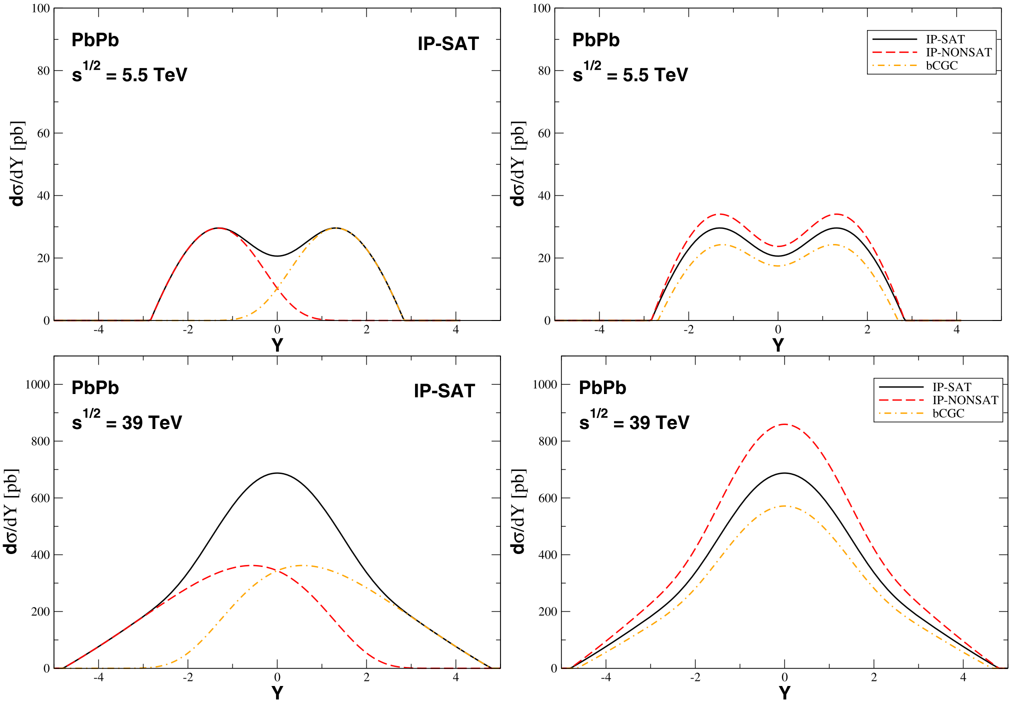

Fig. 4. Rapidity distributions for the exclusive Z^0 photoproduction in $PbPb$ collisions at the LHC (upper panels) and FCC (lower panels) energies. Right panels: Comparison between the predictions derived using the different color dipole models; Left panels: The photon - Pomeron (red dashed) and Pomeron - photon (orange dot-dashed) contributions for the rapidity distributions. The black solid line represents the sum of both contributions.

quence, we have that the rapidity distributions for $PbPb$ collisions are narrower in comparison to pp. In Fig. 4 (left panels) we present the photon – Pomeron and Pomeron – photon contributions, as well the sum of both contributions, derived using the dipole – scattering amplitude given by Eq. (9) and the IP-SAT model as input. We have that the distribution at midrapidities and FCC energy is a factor ≥ 30 in comparison to the prediction for the LHC energy. In Fig. 4 (right panels) we present a comparison between the IP-SAT predictions and those derived using the IP-NONSAT and bCGC models as input to estimate $\mathcal{N}_A(x, \boldsymbol{r}, \boldsymbol{b}_A)$. As in the pp case, the bCGC model provides a lower bound for the exclusive Z^0 photoproduction and the IP-SAT and IP-NONSAT predictions are similar.

Let us now consider pPb collisions. In this case the rapidity distribution is given by sum of the $\gamma p \rightarrow Z^0 p$ and $\gamma Pb \rightarrow Z^0 Pb$ contributions, with the photon being generated by the nucleus and by the proton, respectively. The γp contribution is dominant because the equivalent photon spectrum of the nucleus is enhanced by a factor Z^2 in comparison to the proton one. Consequently, the rapidity distribution is asymmetric with respect to $Y = 0$. One advantage of the study of pPb collisions is that the analysis of the rapidity distribution for a given value of Y gives direct access to the value of x probed in the scattering amplitude, in contrast to symmetric collisions, which receive contributions of the QCD dynamics at small and large values of x. As the behavior of $\mathcal{N}_h$ at large - x is not under theoretical control, it has direct impact on the color dipole predictions for symmetric collisions. An asymmetric distribution is observed in

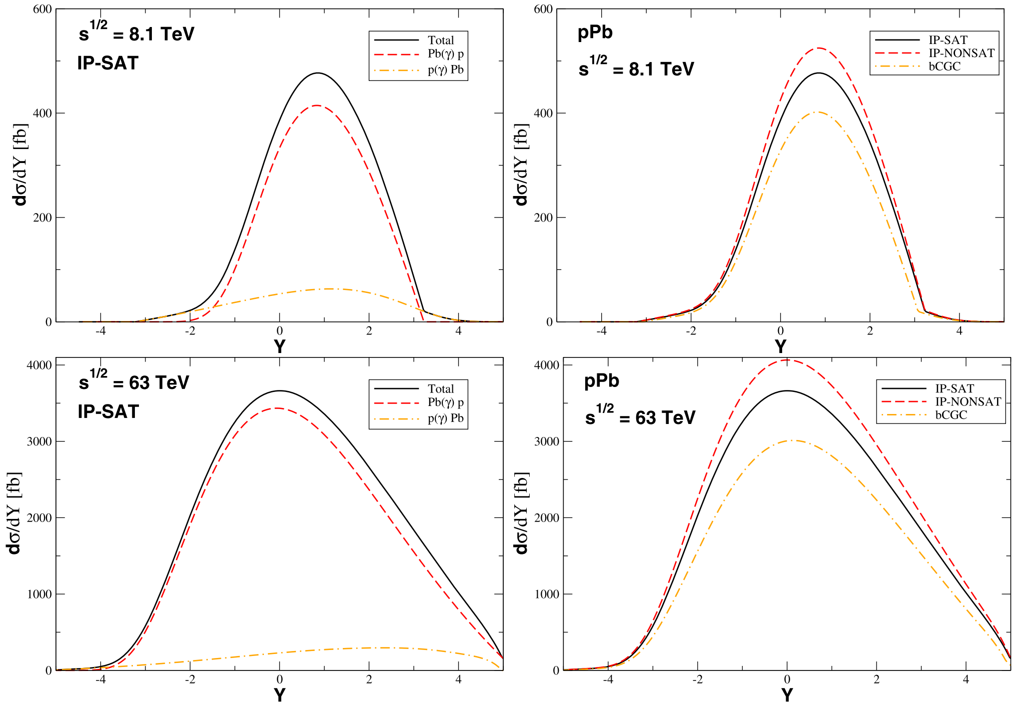

Fig. 5. Rapidity distributions for the exclusive Z^0 photoproduction in pPb collisions at the LHC (upper panels) and FCC (lower panels) energies. Right panels: Comparison between the predictions derived using the different color dipole models; Left panels: The $\gamma p \rightarrow Z^0 p$ (red dashed) and $\gamma Pb \rightarrow Z^0 Pb$ (orange dot-dashed) contributions for the rapidity distributions are presented separately. The black solid line represents the sum of both contributions.

Fig. 5, where we present our predictions for the exclusive Z^0 photoproduction in pPb collisions at $\sqrt{s} = 8.1$ and 63 TeV. In Fig. 5 (left panels) we present the $\gamma p \rightarrow Z^0 p$ (red dashed) and $\gamma Pb \rightarrow Z^0 Pb$ (orange dot-dashed) contributions for the rapidity distributions, as well as the sum of both contributions (black solid), derived using the IP-SAT model. As expected, the distribution is dominated by γp interactions, but the contribution of the γPb interactions is non-negligible at forward rapidities. We have that the prediction for the FCC energy is a factor ≥ 7 larger than the result for the LHC. In Fig. 5 (right panels) we present a comparison between the IP-SAT predictions and those derived using the IP-NONSAT and bCGC models. As in the previous cases, the bCGC model predict the smaller values for the rapidity distributions. Moreover, we have that the contribution of the saturation effects is large at central and forward rapidities.

Finally, let's estimate the cross sections for the exclusive Z^0 photoproduction in pp, pPb and $PbPb$ collisions at the LHC and FCC energies considering two ranges of rapidities: $|Y| \leq 2$ (central rapidities) and $+2 \leq Y \leq +4.5$ (forward rapidities). The predictions for LHC and FCC energies are presented in the Tables 1 and 2, respectively. As expected from the analysis of the rapidity distributions, we have that the predictions increase with the energy and are larger for $PbPb$ collisions. At the LHC energy, central rapidities and pp collisions, we predict cross sections of few fb. For the FCC energy, these predictions increase by a factor ≥ 3. In contrast, for forward rapidities, this increasing is a factor larger than 5. Moreover, our results for pPb collisions indicate that the analysis of the exclusive Z^0 photoproduction can be useful to con-

Table 1
Cross sections in fb for the exclusive Z^0 photoproduction in $pp/pPb/PbPb$ collisions for $\sqrt{s} = 14/8.1/5.5$ TeV and different rapidity ranges.

Model	pp		pPb		$PbPb$	
	$-2.0 \leq Y \leq +2.0$	$+2.0 \leq Y \leq +4.5$	$-2.0 \leq Y \leq +2.0$	$+2.0 \leq Y \leq +4.5$	$-2.0 \leq Y \leq +2.0$	$+2.0 \leq Y \leq +4.5$
bCGC	2.51	0.61	1007.68	174.60	84.81×10^3	6.37×10^3
IP-SAT	3.01	0.78	1202.25	241.24	103.46×10^3	10.49×10^3
IP-NONSAT	3.13	0.80	1362.32	250.72	114.56×10^3	11.88×10^3

Table 2
Cross sections in fb for the exclusive Z^0 photoproduction in $pp/pPb/PbPb$ collisions for $\sqrt{s} = 100/63/39$ TeV and different rapidity ranges.

Model	pp		pPb		$PbPb$	
	$-2.0 \leq Y \leq +2.0$	$+2.0 \leq Y \leq +4.5$	$-2.0 \leq Y \leq +2.0$	$+2.0 \leq Y \leq +4.5$	$-2.0 \leq Y \leq +2.0$	$+2.0 \leq Y \leq +4.5$
bCGC	8.92	4.08	10.45×10^3	3.36×10^3	1.83×10^6	0.33×10^6
IP-SAT	11.17	5.38	12.81×10^3	4.08×10^3	2.20×10^6	0.40×10^6
IP-NONSAT	12.34	6.45	13.7×10^3	4.33×10^3	2.29×10^6	0.44×10^6

strain the underlying assumptions for the QCD dynamics. One important question is the number of events associated to these cross sections. For the typical pp collisions at the LHC, the integrated luminosity per year is expected to be ≈ 1 fb^{-1}, which implies some few events per year. Considering that the experimental search of the Z^0 will probably to rely on the clean leptonic Z^0 decay modes ($Z^0 \rightarrow l^+l^-$), which reduces the number of events in approximately one order of magnitude, we have that the analysis of the exclusive Z^0 photoproduction in pp collisions at the LHC will not be feasible. On the other hand, for the high – luminosity LHC [33,34], where the integrated luminosity per year is expected to ≈ 350 fb^{-1}, we predict ≥ 30 events per year. The analysis of these few events can be used to improve the upper bound for the $\gamma p \rightarrow Z^0 p$ derived by the CDF Collaboration [32]. In the case of pp collisions at the FCC, the integrated luminosity per year is expected to be ≥ 1000 fb^{-1}, which implies that the associated number of events will be $\geq 800\,(400)$ considering the central (forward) rapidity range and the dilepton decay mode. The analysis of these events can be used, in principle, to discriminate between the different approaches for the QCD dynamics. For the nuclear reactions, we predict that the number of events at the LHC will be smaller than one event per year. In contrast, for the FCC energy, the number of events per year is predicted to be ≈ 10. A future search of these events in pPb collisions can be useful to establish an upper bound in the photoproduction cross section.

Some comments are in order. We have verified that our predictions for the $\gamma p \rightarrow Z^0 p$ cross section are similar to the results derived in Refs. [28–31] for small photon – proton center – of – mass energies. Such result is expected since at small energies the cross section is dominated by the two – gluon exchange. On the other hand, at larger energies, the predictions become sensitive to the treatment of the higher order corrections associated to the QCD dynamics, which were treated in different ways in the present paper and in Refs. [29–31]. In particular, in the present study we considered the updated descriptions of the dipole – proton scattering amplitude, which have its free parameters adjusted using the high precision HERA data for inclusive and exclusive ep processes. Such models surpass the previous versions used in Refs. [29,30]. In comparison to the results presented in Refs. [29–31], we predict slightly smaller cross sections. Another important comment is regarding to the background associated to the $\gamma\gamma \rightarrow l^+l^-$ reaction, which can be significant if the $Z^0 \rightarrow l^+l^-$ decay mode is considered to separate the exclusive Z^0 events. In both cases we will have a dilepton pair, two intact hadrons and two rapidity gaps in the final state. In the two – photon fusion, the dileptons will be produced copiously, predominantly at low invariant mass [63]. In contrast, in the leptonic Z^0 decay, the pair have an invariant mass equal to Z^0 mass, with the transverse momenta of each lepton being very large. Moreover, in order to suppress the $\gamma\gamma$ contribution, a cutoff in the transverse momentum of the leading hadrons can be considered. In the exclusive production we have that the typical transverse momentum of the Z^0 in the final state is determined by the transferred momentum in the Pomeron - proton vertex, which is larger than that present in the photon - proton vertex. Consequently, we expect that a different transverse momentum distribution of the scattered hadrons, with exclusive events being characterized by larger values. Such distinct characteristics can be used to suppress the background associated to the two – photon fusion. Finally, we can compare our predictions for the exclusive Z^0 photoproduction with the results derived in Refs. [64,65] for the inclusive reaction, $\gamma p \rightarrow Z^0 X$, where the proton target dissociates. We have that the inclusive cross section is a factor $\approx 10^2$ larger than the exclusive one. However, the background associated to this process can be fully eliminated by imposing the tagging of the protons in the final state by the forward detectors.

4. Conclusions

In this paper we have investigated the exclusive Z^0 photoproduction in pp, pPb and $PbPb$ collisions for the energies of the LHC and of the proposed Future Circular Collider, motivated by the expectation that this process may allow us to probe the description of the QCD dynamics at high energies. We have updated and improved previous studies and presented, for the first time, the predictions for the FCC. In particular, we have taken into account the corrections to the overlap function between the photon and Z^0 wave functions associated to the fact that the outgoing Z^0 has a timelike virtuality $q^2 = M_Z^2 > 0$, as well as we have derived our predictions using the more recent color dipole models for the dipole – proton scattering amplitude, which describe the precise HERA data for the inclusive and exclusive observables and take into account the corrections associated to the DGLAP evolution. Such aspects are important to derive more precise predictions for the Z^0 photoproduction. Our results indicate that the analysis of this final state at the LHC will be a hard task. In contrast, for the FCC energy, the study of this final state is, in principle, feasible in pp collisions. Such future experimental analysis can be useful to complement the study of the QCD dynamics in the exclusive vector meson photoproduction and test the universality of the color dipole formalism.

Declaration of competing interest

The authors declare that they have no known competing financial interests or personal relationships that could have appeared to influence the work reported in this paper.

Acknowledgements

VPG acknowledges useful discussions with M. Rangel, J.D. Tapia-Takaki and W. Schafer. This work was partially financed by the Brazilian funding agencies CNPq, CAPES and INCT-FNA (process number 464898/2014-5).

References

[1] T. Aaltonen, et al., CDF Collaboration, Phys. Rev. Lett. 102 (2009) 242001.
[2] C. Adler, et al., STAR Collaboration, Phys. Rev. Lett. 89 (2002) 272302.
[3] S. Afanasiev, et al., PHENIX Collaboration, Phys. Lett. B 679 (2009) 321.
[4] B. Abelev, et al., ALICE Collaboration, Phys. Lett. B 718 (2013) 1273.
[5] E. Abbas, et al., ALICE Collaboration, Eur. Phys. J. C 73 (2013) 2617.
[6] R. Aaij, et al., LHCb Collaboration, J. Phys. G 40 (2013) 045001.
[7] R. Aaij, et al., LHCb Collaboration, J. Phys. G 41 (2014) 055002.
[8] R. Aaij, et al., LHCb Collaboration, J. High Energy Phys. 1509 (2015) 084.
[9] R. Aaij, et al., LHCb Collaboration, J. High Energy Phys. 1810 (2018) 167.
[10] J. Adams, et al., STAR Collaboration, Phys. Rev. C 70 (2004) 031902.
[11] V. Khachatryan, et al., CMS Collaboration, Phys. Lett. B 772 (2017) 489.
[12] A.M. Sirunyan, et al., CMS Collaboration, Eur. Phys. J. C 79 (8) (2019) 702.
[13] A.M. Sirunyan, et al., CMS Collaboration, Eur. Phys. J. C 79 (3) (2019) 277.
[14] K. Akiba, et al., LHC Forward Physics Working Group Collaboration, J. Phys. G 43 (2016) 110201.
[15] V.P. Goncalves, C.A. Bertulani, Phys. Rev. C 65 (2002) 054905.
[16] V.P. Goncalves, M.V.T. Machado, Eur. Phys. J. C 40 (2005) 519.
[17] F. Gelis, E. Iancu, J. Jalilian-Marian, R. Venugopalan, Annu. Rev. Nucl. Part. Sci. 60 (2010) 463;
H. Weigert, Prog. Part. Nucl. Phys. 55 (2005) 461;
J. Jalilian-Marian, Y.V. Kovchegov, Prog. Part. Nucl. Phys. 56 (2006) 104.

[18] V.P. Goncalves, M.V.T. Machado, Phys. Rev. C 73 (2006) 044902;
V.P. Goncalves, M.V.T. Machado, Phys. Rev. D 77 (2008) 014037;
V.P. Goncalves, M.V.T. Machado, Phys. Rev. C 84 (2011) 011902.
[19] V.P. Goncalves, B.D. Moreira, F.S. Navarra, Phys. Rev. C 90 (2014) 015203;
V.P. Goncalves, B.D. Moreira, F.S. Navarra, Phys. Lett. B 742 (2015) 172;
V.P. Goncalves, B.D. Moreira, F.S. Navarra, Phys. Rev. D 95 (5) (2017) 054011.
[20] W. Schafer, A. Szczurek, Phys. Rev. D 76 (2007) 094014;
A. Rybarska, W. Schafer, A. Szczurek, Phys. Lett. B 668 (2008) 126;
A. Cisek, W. Schafer, A. Szczurek, Phys. Rev. C 86 (2012) 014905;
A. Cisek, W. Schafer, A. Szczurek, J. High Energy Phys. 1504 (2015) 159.
[21] L. Frankfurt, V. Guzey, M. Strikman, M. Zhalov, J. High Energy Phys. 0308 (2003) 043;
V. Guzey, M. Zhalov, J. High Energy Phys. 1310 (2013) 207;
V. Guzey, M. Zhalov, J. High Energy Phys. 1402 (2014) 046.
[22] S.P. Jones, A.D. Martin, M.G. Ryskin, T. Teubner, J. High Energy Phys. 1311 (2013) 085;
S.P. Jones, A.D. Martin, M.G. Ryskin, T. Teubner, Eur. Phys. J. C 76 (11) (2016) 633.
[23] V.P. Goncalves, M.V.T. Machado, B.D. Moreira, F.S. Navarra, G.S. dos Santos, Phys. Rev. D 96 (9) (2017) 094027.
[24] N. Armesto, A.H. Rezaeian, Phys. Rev. D 90 (5) (2014) 054003.
[25] J. Cepila, J.G. Contreras, J.D. Tapia Takaki, Phys. Lett. B 766 (2017) 186;
J. Cepila, J.G. Contreras, M. Krelina, Phys. Rev. C 97 (2) (2018) 024901;
J. Cepila, J.G. Contreras, M. Krelina, J.D. Tapia Takaki, Nucl. Phys. B 934 (2018) 330.
[26] V.P. Goncalves, F.S. Navarra, D. Spiering, Phys. Lett. B 768 (2017) 299.
[27] V.P. Goncalves, F.S. Navarra, D. Spiering, Phys. Lett. B 791 (2019) 299.
[28] J. Pumplin, arXiv:hep-ph/9612356.
[29] V.P. Goncalves, M.V.T. Machado, Eur. Phys. J. C 56 (2008) 33, Eur. Phys. J. C 61 (2009) 351 (Erratum).
[30] L. Motyka, G. Watt, Phys. Rev. D 78 (2008) 014023.
[31] A. Cisek, W. Schafer, A. Szczurek, Phys. Rev. D 80 (2009) 074013.
[32] T. Aaltonen, et al., CDF Collaboration, Phys. Rev. Lett. 102 (2009) 222002.
[33] A. Abada, et al., FCC Collaboration, Eur. Phys. J. C 79 (6) (2019) 474.
[34] A. Abada, et al., FCC Collaboration, Eur. Phys. J. Spec. Top. 228 (4) (2019) 755.
[35] A. Abada, et al., FCC Collaboration, Eur. Phys. J. Spec. Top. 228 (5) (2019) 1109.
[36] C.A. Bertulani, G. Baur, Phys. Rep. 163 (1988) 299;
F. Krauss, M. Greiner, G. Soff, Prog. Part. Nucl. Phys. 39 (1997) 503;
G. Baur, K. Hencken, D. Trautmann, J. Phys. G 24 (1998) 1657;
G. Baur, K. Hencken, D. Trautmann, S. Sadovsky, Y. Kharlov, Phys. Rep. 364 (2002) 359;
C.A. Bertulani, S.R. Klein, J. Nystrand, Annu. Rev. Nucl. Part. Sci. 55 (2005) 271;
V.P. Goncalves, M.V.T. Machado, J. Phys. G 32 (2006) 295;
A.J. Baltz, et al., Phys. Rep. 458 (2008) 1;
J.G. Contreras, J.D. Tapia Takaki, Int. J. Mod. Phys. A 30 (2015) 1542012.
[37] G. Gil da Silveira, V.P. Goncalves, M.M. Jaime, Phys. Rev. D 95 (3) (2017) 034020.
[38] V.M. Budnev, I.F. Ginzburg, G.V. Meledin, V.G. Serbo, Phys. Rep. 15 (1975) 181.
[39] M. Drees, D. Zeppenfeld, Phys. Rev. D 39 (1989) 2536.
[40] A. Caldwell, H. Kowalski, Phys. Rev. C 81 (2010) 025203.
[41] T. Lappi, H. Mantysaari, Phys. Rev. C 83 (2011) 065202.
[42] H. Mantysaari, B. Schenke, Phys. Rev. Lett. 117 (5) (2016) 052301.
[43] M. Krelina, V.P. Goncalves, J. Cepila, Nucl. Phys. A 989 (2019) 187.
[44] N.N. Nikolaev, B.G. Zakharov, Phys. Lett. B 332 (1994) 184;
N.N. Nikolaev, B.G. Zakharov, Z. Phys. C 64 (1994) 631.
[45] Y. Hatta, B.W. Xiao, F. Yuan, Phys. Rev. D 95 (11) (2017) 114026.
[46] R. Fiore, V.R. Zoller, JETP Lett. 82 (2005) 385, Pis'ma Zh. Eksp. Teor. Fiz. 82 (2005) 440.
[47] H. Kowalski, L. Motyka, G. Watt, Phys. Rev. D 74 (2006) 074016.
[48] A.H. Rezaeian, I. Schmidt, Phys. Rev. D 88 (2013) 074016.
[49] E. Levin, K. Tuchin, Nucl. Phys. A 691 (2001) 779.
[50] H. Kowalski, D. Teaney, Phys. Rev. D 68 (2003) 114005.
[51] H. Mantysaari, P. Zurita, Phys. Rev. D 98 (2018) 036002.
[52] K. Golec-Biernat, M. Wusthoff, Phys. Rev. D 59 (1999) 014017.
[53] M.S. Kugeratski, V.P. Goncalves, F.S. Navarra, Eur. Phys. J. C 46 (2006) 465;
M.S. Kugeratski, V.P. Goncalves, F.S. Navarra, Eur. Phys. J. C 46 (2006) 413.

[54] K. Kutak, J. Kwiecinski, Eur. Phys. J. C 29 (2003) 521.
[55] J. Jalilian-Marian, Phys. Rev. D 68 (2003) 054005, Phys. Rev. D 70 (2004) 079903 (Erratum).
[56] V.P. Goncalves, P. Hepp, Phys. Rev. D 83 (2011) 014014;
V.P. Gonçalves, D.R. Gratieri, Phys. Rev. D 88 (1) (2013) 014022;
V.P. Gonçalves, D.R. Gratieri, Phys. Rev. D 90 (5) (2014) 057502.
[57] J.L. Albacete, J.I. Illana, A. Soto-Ontoso, Phys. Rev. D 92 (1) (2015) 014027.
[58] E. Iancu, K. Itakura, L. McLerran, Nucl. Phys. A 708 (2002) 327.
[59] A.M. Stasto, K.J. Golec-Biernat, J. Kwiecinski, Phys. Rev. Lett. 86 (2001) 596.
[60] H. Kowalski, T. Lappi, R. Venugopalan, Phys. Rev. Lett. 100 (2008) 022303.
[61] H. Kowalski, T. Lappi, C. Marquet, R. Venugopalan, Phys. Rev. C 78 (2008) 045201.
[62] E.R. Cazaroto, F. Carvalho, V.P. Goncalves, F.S. Navarra, Phys. Lett. B 671 (2009) 233.
[63] C. Azevedo, V.P. Goncalves, B.D. Moreira, Eur. Phys. J. C 79 (5) (2019) 432.
[64] M. Hayashi, K. Katsuura, Prog. Theor. Phys. 61 (1979) 1166.
[65] C.S. Kim, W.J. Stirling, Z. Phys. C 53 (1992) 601.